FOUNTAIN JOURNAL OF NATURAL & APPLIED SCIENCES

A Publication of the College of Natural & Applied Sciences

Fountain University, Osogbo, Nigeria

Application of aeroradiometric data for lithological classification and iron ore prospecting in southwestern Nigeria

Ojulari, B.A.*, Olatunji, S., Folorunsho, I.O.

Department of Geophysics, University of Ilorin, Ilorin, Nigeria

**Correspondence:* 12-68et003pg@students.unilorin.edu.ng

ABSTRACT

The efforts to diversify the economy make it imperative to develop Nigeria's solid mineral sector. Geological mapping represents a critical foundation in solid mineral prospecting. The integration of aeroradiometric data into reconnaissance geological mapping of iron ore occurrence in parts of Sheet 224 (Osi), Nigeria, provides complementary information on alteration zones, intrusions, and lithological units. Analysis of aeroradiometric data for the study area reveals that the total count (TC) value ranges from 7.7 to 77.1 counts per thousand (cpt). Additionally, the potassium (K) concentration ranges from 0.2% to 5.0%. Also, the ranges of equivalent values of Thorium (eTh) and Uranium (eU) are 6.5 ppm to 68.6 ppm and 0.8 ppm to 10.1 ppm, respectively. The synthesis of results from TC, K, eTh, and eU maps reveals the presence of metasediments, metasedimentary rocks, and intrusive rocks in the study area. Additionally, post-metamorphic tectonic activities in the study area are indicated by the presence of mafic and felsic intrusive rocks in the western and eastern parts. The K/eTh map reveals the presence of hydrothermal alteration zones in the eastern part of the study area, where the eTh and eU maps confirm the presence of mafic intrusive rock. Hence, the occurrence of iron ore in this area is inferred.

ARTICLE INFO

Article history:
Received July 2025
Revised September 2025
Accepted September 2025

Keywords:
Aeroradiometric Survey, Lithological Mapping, Hydrothermal Alteration, Mineral Prospecting

Introduction

The clamour for economic diversification to reduce over-dependence on revenue from petroleum products makes it imperative to develop Nigeria's solid mineral sector. Mineral resources are beneficial materials occurring in the earth in sufficient quantity and adequate quality to be extracted for economic benefit [1]. Nigeria is richly endowed with mineral resources, which include the liquid fuels (petroleum) and the
solid minerals such as bitumen and coal [2]. Additionally, numerous valuable solid mineral resources, including gold, tin, lithium, and iron ore, have been identified across various locations in Nigeria (Fig. 1). However, these resources are largely underdeveloped due to a greater focus on the petroleum sector. Successive governments have implemented policies to encourage the development of the solid minerals sector of the Nigerian economy to improve its contribution to the Gross Domestic Product (GDP) [3]. Consequently, the Nigerian Mining Sector increased its contribution to the Nation's GDP, having contributed 0.85% in 2022 (2021: 0.63%), representing a 32% year-on-year growth over 2021 [4]. Iron ore is one of the several solid mineral resources found in locations across Nigeria. It ranks second only to oil in global economic importance, although it is often overshadowed by crude oil in popular discourse [5]. Generally, solid mineral deposits occur within a metallogenic province, which is a large geographic area characterised by a specific concentration and type of mineral deposits. These provinces are defined by the presence of economically significant mineral deposits formed during a particular geological epoch

DOI: https://doi.org/10.53704/fujnas.v14i1.1024

and within a specific tectonic setting. Hence, geological mapping is always essential in solid mineral prospecting.

The aeroradiometric method has been used extensively for geological mapping and mineral exploration in many parts of the world. This is because all rocks and soils are naturally radioactive and contain varying proportions of various radioactive elements [6]. Therefore, the aeroradiometric method distinguishes different rock types based on the type and quantity of emission measured over each rock type. Hence, it is applicable to gross geologic mapping. It can also assist in mapping intrusive-related solid mineral ores and potential zones of mineralisation. This is because the concentration of radioelements in rocks is affected by mineralisation processes. Additionally, the concentration and distribution of radioactive elements in rocks are influenced by differences in lithology and the geochemical processes of rock formation. Therefore, integrating aeroradiometric data into geological studies provides complementary information on alteration zones, lithological units, geological structures, and mineral resource potential across large areas.

Furthermore, significant improvements in geophysical data resolution, enabled by advanced data processing and image analysis techniques, have enabled the discovery of subtle variations in geophysical responses associated with geological features [7]. Hence, to support economic diversification, this study used aeroradiometric mapping for identifying lithological units and alteration zones with the potential for iron ore mineralization in the study area.

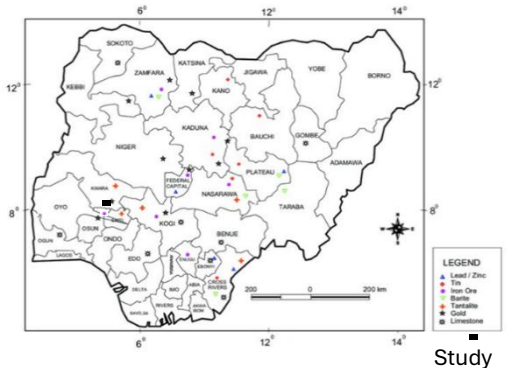

Figure 1: Locations of various mineral mining sites in Nigeria

Description of the study area

Location

The area of study is located between latitudes 8^0 13'0''N and 8^0 23'0''N and between longitudes $5^0$0'00'E and $5^0$14'00'E. It has a total area of about 607 square kilometres (Fig. 1). Accessibility is provided through a network of major and minor roads. The Ajase Ipo-Omu Aran road is a major road through the study area. Several minor roads, such as the Oke Onigbin-Owu Isin-Owa Onire Road, Isanlu Isin-Omu Aran, and Omu Aran -Olla- Oro Ago-Owa Kajola road, facilitate mapping in the study area. Many footpaths also enhance accessibility in the study area.

Climate, vegetation and drainage

The study area experiences two distinct seasons annually. These are the wet and dry seasons. The wet season runs from April to October. Also, the dry season lasts from November to March [8]. The total annual rainfall in the study area ranges from 1270 mm to 1524 mm. The temperature range in the study area is about 30 °C (min) to 35 °C (max) [9].

The vegetation of the study area forms an ecotonal zone between the humid lowland rainforest of Southwestern Nigeria and the Guinea savannah of North-Central Nigeria. The plant assemblage is characterised by dispersed arboreal species interspersed with tall shrubs. Hydrologically, the landscape is primarily influenced by the River Awere and its tributaries, which exhibit a predominantly dendritic drainage pattern.

Geological setting

The area of study is located within the basement complex of southwestern Nigeria. The geology of Nigeria can be further divided into four main metallogenic provinces (Fig. 2). The metallogenic framework of Nigeria is delineated by four major provinces, characterised by distinct tectono-magmatic events and mineralisation processes. These include the Sn–Ta–Nb pegmatite belt of Late Pan-African age, which is economically significant for rare-metal mineralization; the Jurassic Sn–Nb–Ta Younger Granite province, related to anorogenic magmatism; the Cretaceous Pb–Zn province of the Benue Trough, which hosts extensive stratabound sulphide deposits; and the Au province of Western Nigeria, noted for its auriferous mineralization linked to Precambrian basement structures. These provinces are associated with specific types of mineral deposits, rock types, geological ages and tectonic settings. In Southwestern Nigeria, evidence of at least four distinct thermotectonic episodes has been recognised. The development of a planar

DOI: https://doi.org/10.53704/fujnas.v14i1.1024

penetrative fabric represents the earliest phase. This was followed by a fold-forming event characterised by the formation of F_1 folds. A subsequent phase of deformation refolded the F_1 structures, forming the F_2 fold system. The final episode is marked by shear deformation, which gave rise to both minor and major dextral and sinistral faults, as well as the development of a prominent shear zone and associated fault systems [11].

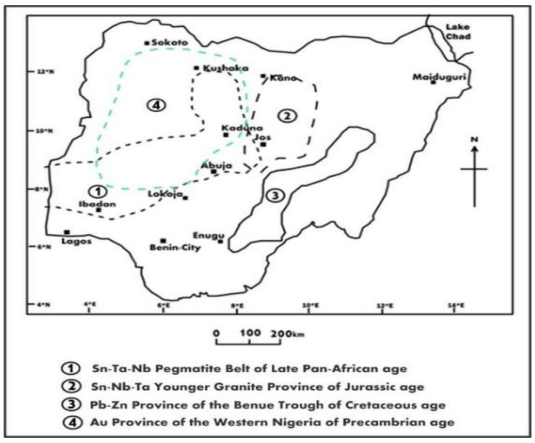

Figure 2: Metallogenic Province of Nigeria [10]

Materials and Methods

This study utilised aeroradiometric data from Sheet 224 (Osi), as obtained from the Nigerian Geological Survey Agency (NGSA). The aeroradiometric data served as a basis for subsequent ground validation, detailed geophysical investigations, and quantitative reserve evaluation. The aeroradiometric data were acquired by the Nigerian Geological Survey Agency (NGSA) during a nationwide airborne geophysical survey that simultaneously collected aeromagnetic, electromagnetic, and radiometric datasets. This survey, conducted between 2003 and 2012 by Fugro Airborne Surveys on behalf of NGSA, generated a comprehensive geophysical database for Nigeria. During data acquisition, magnetic, electromagnetic, and radiometric measurements were systematically recorded and compiled into a national geoscientific database. The data were made available in Geosoft grids at a 1:100,000 scale, as well as in half-degree sheets and ASCII files. Radiometric surveying entails the measurement of naturally occurring Uranium (eU), Potassium (%K), and Thorium (eTh), which occur as trace elements within rock-forming minerals and soil profiles. These elements undergo radioactive decay, releasing gamma radiation that can be detected and quantified for geoscientific interpretation [12]. Aeroradiometric surveys record gamma radiation emitted by naturally occurring radioactive elements, including potassium (K), uranium (U), and thorium (Th). These datasets yield a characteristic geochemical signature of the Earth's surface, which supports the differentiation of lithological units (Table 1) and the recognition of alteration zones frequently associated with mineralisation [13]. The data were gridded in Oasis Montaj version 8.4 at a 125 m cell size using line spacing and minimum curvature interpolation, followed by micro-levelling and basic filtering to improve data quality.

Radiometric maps developed from the analysis of aeroradiometric data include the total count (TC) (cpt) map, K (%) map, eTh (ppm) map, eU (ppm) map, K/Th ratio map, and ternary image map. These maps were interpreted for gross lithological discrimination and hydrothermal zone identification using Killeen's classification [14].

Visual interpretation was used to classify each map into high-concentration zone (red-purple), intermediate-concentration zone (green-yellow), and low-concentration zone (light blue-deep blue) based on the coloured legend for each map. Interpretation of the aero-radiometric data was done based on the radioelement concentration of different classes of rocks by Killeen [14] (Table 1).

Results and Discussion

The total count contour map (Fig. 3) delineates three distinct radiometric zones within the study area. A high concentration (25.6–77.1 cpt) occurs in the eastern sector, trending NE–SW, and is associated with metamorphic rocks. The metamorphic units coincide with deformation zones where hydrothermal alteration can enrich hematite and magnetite, indicative of a probable zone of iron ore mineralisation [15, 16].

An intermediate concentration (15.2–25.6 cpt) characterises the western sector, corresponding to older granites, meta-sediments, and meta-gabbro. In contrast, low concentrations (7.7–15.2 cpt) are predominantly confined to the northwestern and southwestern parts of the area, reflecting weak radiometric signatures associated with felsic intrusive rocks with limited alteration potential [17] and a low prospect for iron ore mineralisation.

The potassium (K) map (Fig. 4) reveals high concentration (HC) values ranging from 1.1% to 5.0% are prominent in the southeastern and northeastern portions of the study area. These anomalies

DOI: https://doi.org/10.53704/fujnas.v14i1.1024

Table 1. Radioelement Concentration in different Classes of Rocks [14]

Rock Type	Potassium (%)		Uranium (ppm)		Thorium (ppm)	
	Mean	Range	Mean	Range	Mean	Range
Felsic Extrusives	3.1	1.0 - 6.2	4.1	0.8-16.4	11.9	1.1-41.0
Felsic Intrusives	3.4	0.1-7.6	4.5	0.1-30.0	25.7	0.1-253.1
Intermediate Extrusives	1.1	1.1-2.5	1.1	0.2-2.6	2.4	0.4-6.4
Intermediate Intrusives	2.1	0.1-6.2	3.2	0.1-23.4	12.2	0.4-106.0
Mafic Extrusives	0.7	0.06-2.4	0.8	0.03-3.3	2.2	0.05-8.8
Mafic Intrusives	0.8	0.01-2.6	0.8	0.01-5.7	2.3	0.03-15.0
Ultramafic	0.3	0-0.8	0.3	0-1.6	1.4	0-7.5
Alkali Feldspathoidal Intermediate Intrusives	6.5	2.0-9.0	29.7	1.9-62.0	133.9	9.5-265.0
Alkali Feldspathoidal Mafic Intrusives	4.2	1.0-9.9	55.8	0.3-720.0	132.6	0.4-880.0
Chemical Sedimentary Rocks	0.6	0.02-8.4	3.6	0.03-26.7	14.9	0.03-132.0
Carbonates	0.3	0.01-3.5	2.0	0.03-18.0	1.3	0.03-10.8
Detrital Sedimentary Rocks	1.5	0.01-9.7	4.8	0.01-80.0	12.4	0.2-362.0
Metamorphosed Igneous Rocks	2.5	0.1-6.1	4.0	0.1-148.5	14.8	0.1-104.2
Metamorphosed Sedimentary Rocks	2.1	0.01-5.3	3.0	0.1-53.4	12.0	0.1-91.4

correspond to meta-igneous rocks and display a NE–SW structural trend. The meta-igneous rocks indicate zones of hydrothermal alteration indicative of iron-ore mineralisation comparable to findings of Okoye *et al.* (2012), and Adabanija *et al.* (2020). Both studies show consistent with hydrothermal-related mineralisation [18, 19].

Intermediate concentrations (IC), ranging from 0.4% to 1.1%, together with low concentrations (LC), ranging from 0.2% to 0.4%, are associated with felsic intrusive rocks and are predominantly observed in the western half of the study area. The felsic intrusive rocks exhibit limited alteration potential and are considered to have a low prospect for iron ore mineralization [20].

The equivalent thorium (eTh) map (Fig. 5) reveals high concentration (HC) values ranging from 22.5 ppm to 68.6 ppm in the northeastern and southeastern parts of the study area.

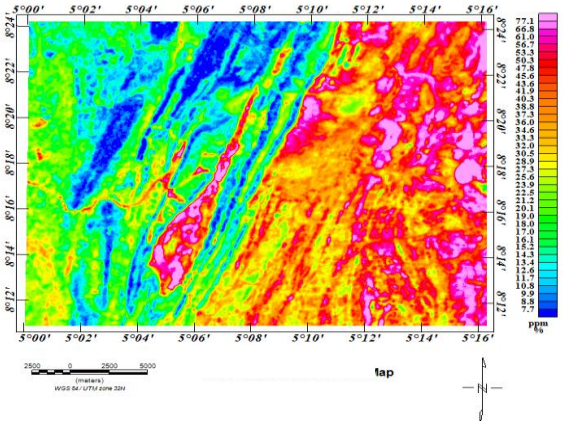

Figure 3: Total Count Contour Map of the Study Area

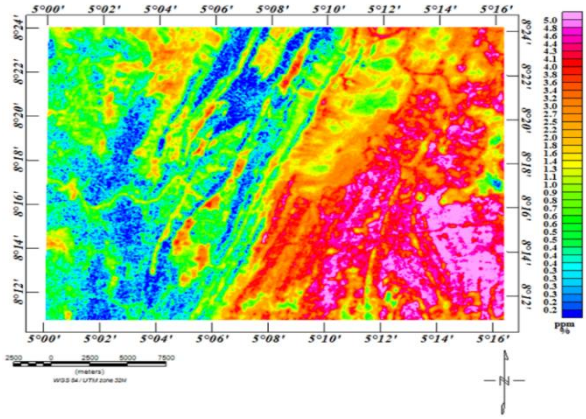

Figure 4: Potassium (K) Map of the Study Area

These are characteristic of mafic intrusive rocks indicative of higher iron-ore mineralisation, consistent with radiometric signatures reported in Nigerian basement complexes [21]. Hence, the equivalent thorium (eTh) map (Fig. 5) shows pronounced iron-ore mineralization potential in the northeastern and southeastern parts of the study area, a pattern that compares favourably with the similarly high-potential zones observed on both the Total Count map (Fig. 3) and the Potassium map (Fig. 4). Intermediate concentrations (IC), ranging from 14.7 ppm to 22.5 ppm, while low concentrations (LC), ranging from 6.5 ppm to 14.7 ppm, occur mainly in the northwestern region and are relatively widespread across the map. These are typically associated with felsic intrusive rocks and low-mineralisation prospects.

The equivalent uranium (eU) map (Fig. 6) shows high-concentration (HC) values of 4.1-10.1 ppm, prominently expressed in the northeastern part of the study area, where they are associated with mafic

DOI: https://doi.org/10.53704/fujnas.v14i1.1024

intrusive rocks suggestive of a hydrothermal alteration zone and iron ore mineralisation. Intermediate concentrations (IC), ranging from 2.4 to 4.1 ppm, and low concentrations (LC), ranging from 0.8 to 2.4 ppm, are associated with felsic intrusive rocks, which are less prospective for iron ore mineralisation.

Elevated potassium (%) in conjunction with depleted thorium concentrations (eTh) is a well-documented geochemical signature of hydrothermal alteration associated with ore-forming systems [22]. Accordingly, the K/eTh ratio map provides an effective tool for delineating alteration zones associated with iron ore mineralisation. Hydrothermal solutions are known to mobilise and concentrate diverse metals and salts, thereby exerting fundamental control over mineralisation processes [23,24]. The K/eTh ratio distribution of the study area is illustrated in Fig. 7. Anomalous zones, depicted in red to pink hues with values ranging from 0.1–0.2 %/ppm, are interpreted as strong indicators (SI) of hydrothermal alteration and hence, probable iron ore mineralisation. These anomalies are predominantly localised within the northwestern and southeastern sectors of the study area and are spatially correlated with metasediments, metavolcanics, metamorphic assemblages, and schist-felsites. In contrast, low-indicator (LI) zones exhibit low K concentrations and elevated eTh values. The alteration anomalies exhibit a dominant NE–SW structural trend, consistent with the regional tectonic framework.

The potassium-to-equivalent uranium (K/eU) ratio map (Fig. 8) shows high-concentration (HC) values ranging from 0.3 to 1.5 ppm, predominantly in the eastern part of the study area, where they are associated with metamorphic rocks. This is comparable to the results obtained in the Potassium/equivalent Thorium map (Fig. 7). Intermediate concentrations (IC), ranging from 0.2 to 0.3 ppm, and low concentrations (LC), spanning 0.1 to 0.2 ppm, are characteristic of meta-igneous and metasedimentary rocks, respectively. Finally, a ternary map of the study area (Fig. 9) was generated by modulating the three primary colours—red (R), green (G), and blue (B)—in equal proportions to enhance radiometric contrasts and enable lithological discrimination. The ternary display effectively illustrates the relative distribution of K, Th, and U, thereby providing a basis for interpreting lithological variations and their association with mineralisation processes. High-level concentrations (HLCs) of radioactive elements, as indicated by strong radiometric responses, are spatially correlated with metasediments, schist-felsites, and metamorphic rocks. These zones extend from latitude 5°06'N in the southwestern sector to approximately latitude 5°12'N in the northeastern part of the study area. Conversely, low-concentration (LC) zones, represented by black tones, are primarily associated with meta-igneous lithologies. In terms of spectral response, red domains reflect elevated K with relatively low Th and U, characteristic of metasedimentary rocks and consistent with areas affected by hydrothermal alteration, as highlighted in the K/eTh ratio map. Green domains indicate high Th coupled with low K and U, and are spatially linked to metavolcanic rocks. The observed distribution pattern demonstrates that alteration zones identified from the ternary image correspond with those revealed by the K/eTh and K/eU ratio maps, particularly along the NE–SW structural trend. This spatial correspondence shows the utility of integrating ternary mapping with ratio analysis for delineating hydrothermal alteration systems and for refining exploration targets in the study area.

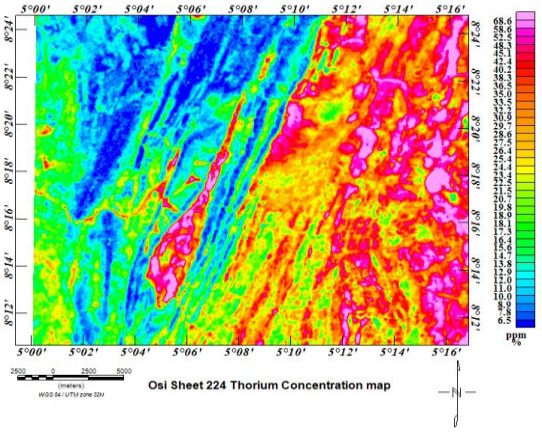

Figure 5: Equivalent Thorium (eTh) Map of the Study Area

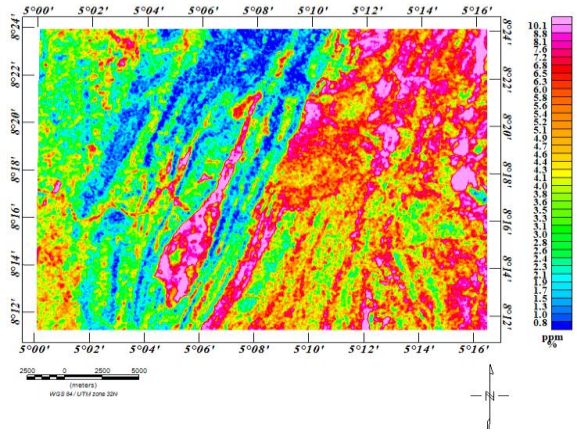

Figure 6: Equivalent Uranium (eU) Map the Study Area

DOI: https://doi.org/10.53704/fujnas.v14i1.1024

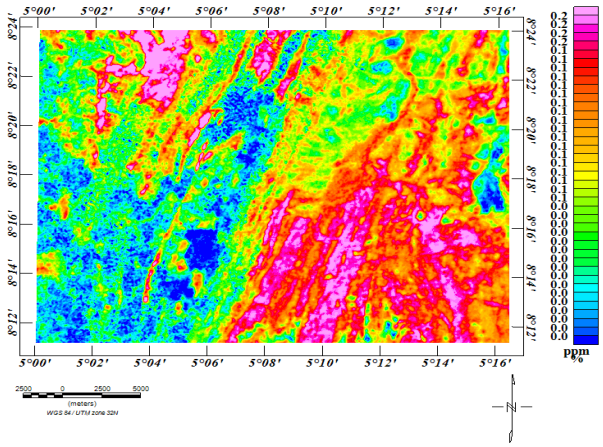

Figure 7: Potassium/equivalent Thorium map (K/eTh) of the Study Area

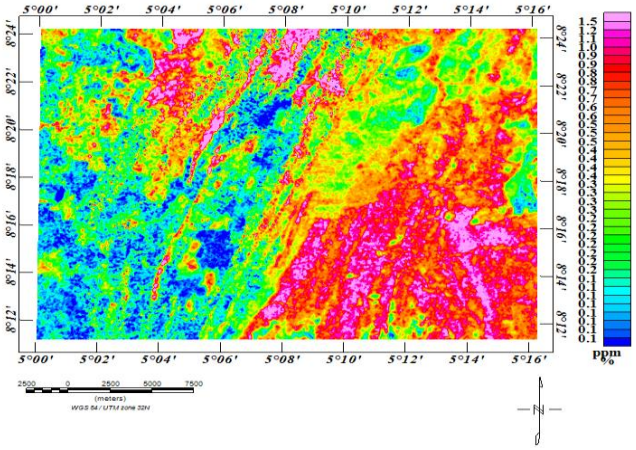

Figure 8: Potassium/equivalent Uranium map (K/eU) of the Study Area

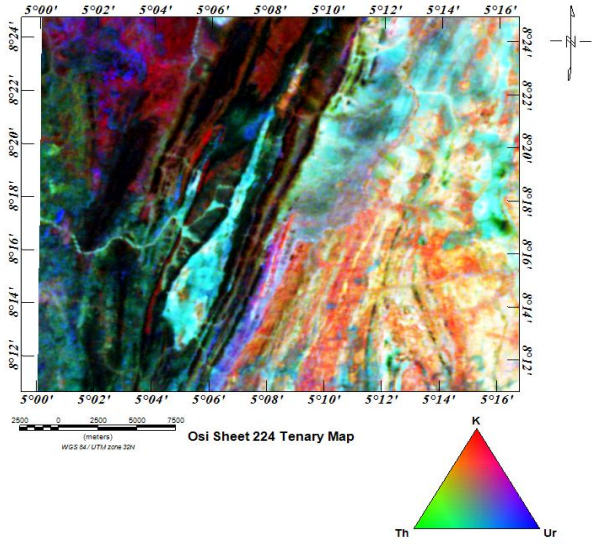

Figure 9: The Ternary Map of the Study Area

Conclusion

The interpretation of aeroradiometric datasets has provided valuable insights into the lithological framework and structural evolution of the study area. Radioelement maps indicate that the terrain is underlain by lithologies of diverse compositions, with the dominant structural orientation trending NE–SW. Integration of the total count (TC), potassium (K), equivalent thorium (eTh), and equivalent uranium (eU) maps reveals that metasedimentary units are concentrated in the western part of the area, whereas meta-igneous rocks dominate the eastern sector. The spatial distribution of mafic and felsic intrusions further reflects a history of regional metamorphism and tectonothermal activity.

The K/eTh ratio map highlights discrete zones of hydrothermal alteration, particularly within the eastern portion of the area, while complementary signatures from the eTh and eU maps confirm the presence of mafic intrusive bodies. These features collectively suggest favourable conditions for mineralisation, with the potential occurrence of iron ore strongly inferred. Therefore, this study recommends more detailed exploration within the area to better characterize the inferred iron ore prospect and to determine its tonnage and grade, with objective of establishing its commercial viability and potential for exploitation.

Acknowledgements

This research is part of the PhD of the corresponding author, supervised by the co-authors. The PhD program of the corresponding author is funded by the Tertiary Education Trust Fund (TETFund) under the Staff Training and Development Award Fund.

Conflicts of Interest Statement

The authors declare that no conflicts of interest are associated with this work. The funding body exercised no influence on the conceptualisation, design, or execution of the study. The preparation and submission of this manuscript were undertaken solely at the discretion of the authors.

References

1. Olade MA. Solid mineral deposits and mining in Nigeria: a sector in transitional change. Achiever J Sci Res. 2019;2(1):1–16.
2. Obaje NG. Geology and mineral resources of Nigeria. Lecture Notes in Earth Sciences. Vol. 120. Berlin: Springer; 2009.

DOI: https://doi.org/10.53704/fujnas.v14i1.1024

3. Ajayi A. KPMG Nigerian Mining Sector Watch. Vol. 5. Lagos: KPMG; 2023.
4. Salihu U. Iron ore and its economic importance in contemporary Nigeria. Raw Materials 360. Abuja: Raw Materials Research and Development Council (RMRDC); 2025. Available from: https://360.rmrdc.gov.ng/iron-ore-and-its-economic-importance-in-contemporary-nigeria/
5. Ford K, Harris JR, Shives R, Carson J, Buckle J. Remote predictive mapping: gamma-ray spectrometry as a tool for mapping Canada's North. Geosci Can. 2008;35(3–4):109–26.
6. Lar UA, Agene JI, Umar AI. Geophagic clay materials from Nigeria: a potential source of heavy metals and human health implications. Environ Geochem Health. 2014;36(5):973–85.
7. Akinsunmade A, Nguyen Dinh C, Wojas A, Tomecka-Suchoń ST. Characterization of lithological zones of the Isanlu sheet 225, North-Central Nigeria, using aerogeophysical datasets. Acta Geophys. 2020;68(3):651–65.
8. Olasehinde PI. Characteristics of rain, groundwater and surface water in Ilorin, Kwara State, Nigeria. Zbl Geol Paläont Teil I. 1999;3–4:149–58.
9. Olabode AD, Ajibade LT. Environment-induced conflict and sustainable development: a case of Fulani–farmers' conflict in Oke-Ero LGA, Kwara State, Nigeria. J Sustain Dev Afr. 2010;12(5):159–73.
10. Woakes M. Basement metallogeny of Northwestern Nigeria. In: Oluyide PO, Mbonu WC, Ogezi AEO, editors. Precambrian Geology of Nigeria. Kaduna: Geological Survey of Nigeria; 1988. p. 183–94.
11. Adedoyin AD, Adekeye JID, Ojo OJ, Bamigboye OS, Ajayi MT. Oke-Ode Dome: a product of fold interference followed by shearing. Scott J Arts Soc Sci Sci Stud. 2013;12(2):100–107.
12. Egwuonwu GN, Ejike KN, Onyekwelu CC. Interpretation of radiometric anomalies over parts of the Lower Benue Trough, Nigeria, using high-resolution aeroradiometric data. Adv J Sci Technol Eng. 2023;3(1):41–50.
13. Ogunsanwo FO, Ayanda JD, Olurin OT, Gbadamosi MR,
14. Osinubi AD, Giwa KW, Ogunneye AL. Lithological characterization of selected river sediments in Ogun State using spectroscopic approaches. J Niger Geophys Soc. 2019;2(1):37–46.
15. Killeen PG. Gamma-ray spectrometric methods in uranium exploration: application and interpretation. In: Hood PJ, editor. Geophysics and Geochemistry in the Search for Metallic Ores. Economic Geology Report 31. Ottawa: Geological Survey of Canada; 1979. p. 163–229.
16. Taylor G, Perez N, Anderson J. Geochemical and structural controls on hydrothermal iron enrichment in metamorphic terrains. J Appl Geosci. 2018;45(2):115–28.
17. Olobaniyi SB, Ogunleye T. Radiometric signatures and mineralization potential of basement complex rocks in Nigeria. Niger J Min Geosci. 2020;56(1):33–47.
18. Odeyemi IB, Kolawole F, Afolayan FO. Petrology and radiometric characteristics of metavolcanic and gabbroic suites in the Nigerian Basement Complex. J Earth Syst Sci. 2019;128(4):1–15.
19. Okoye NO, Amadi AN, Olasehinde PI, Okunlola IA, Alkali YB, Ako TA, et al. Radiometric survey as a useful tool in geological mapping of western Nigeria. J Geogr Geol. 2012;4(1):242–49.
20. Adabanija MA, Anie ON, Oladunjoye MA. Radioactivity and gamma-ray spectrometry of basement rocks in Okene area, southwestern Nigeria. NRIAG J Astron Geophys. 2020;9(1):71–84.
21. Porter TM. Current understanding of iron-oxide-associated alkali-altered (IOCG) systems. PGC Publishing; 2010.
22. Ndatuwong LG. Assessment of radioelement-hosting structures and hydrothermal alteration zones using aeroradiometric data in basement rocks of North-Central Nigeria. Galaxy Int Interdiscip Res J. 2022;10(7):205–14.
23. Ostrovskiy EY. Antagonism of radioactive elements in wall-rock alteration fields and its use in aerogamma-spectrometric prospecting. Int Geol Rev. 1975;17(4):461–68.
24. Boamah D. Application of soil geochemistry to gold exploration in the Birimian rocks of Ghana [MSc thesis]. 1993.
25. Manu J. Gold deposits of Birimian greenstone belts in Ghana: hydrothermal alteration and thermodynamics [PhD thesis]. Braunschweiger Geologisch-Paläontologische Dissertationen, Vol. 17; 1993.

DOI: https://doi.org/10.53704/fujnas.v14i1.1024